ACS APPLIED MATERIALS & INTERFACES

Research Article

www.acsami.org

Highly Fluorescent Amidine/Schiff Base Dual-Modified Polyacrylonitrile Nanoparticles for Selective and Sensitive Detection of Copper Ions in Living Cells

Inkyu Lee,[†] Sojin Kim,[†] Seh-na Kim, Yoonsun Jang, and Jyongsik Jang*

WCU Program of Chemical Convergence for Energy and Environment (C2E2), School of Chemical and Biological Engineering, College of Engineering, Seoul National University, Shinlimdong 56-1, Seoul 151-742, Korea

Supporting Information

ABSTRACT: Highly fluorescent surface modified polyacrylonitrile nanoparticles (PAN NPs) of 50 nm diameter were fabricated for selective Cu^{2+} sensing. After surface modification, the PAN NPs were converted to amidine/Schiff base dual-modified PAN nanoparticles (tPAN NPs) with a Cu^{2+} sensing property and high QY (0.19). The selectivity of tPAN NPs for Cu^{2+} is much higher than that of other metal ions due to the fact that amidine group on the surface of tPAN NPs has a higher binding affinity with Cu^{2+}. The effect of other metal ions on the fluorescence intensity of the tPAN NPs was also studied, and other metal ions showed a low interference response in the detection of Cu^{2+}. Furthermore, as a metal ion chelator, ethylenediaminetetraacetate can competitively interact with Cu^{2+} to recover the quenched fluorescence of tPAN NPs. The tPAN NPs are easily introduced into cells and exhibit low toxicity, enabling their use as a fluorescence sensor for Cu^{2+} in living cells. The tPAN NPs provide a new direction for the development of copper ion sensors in living cells.

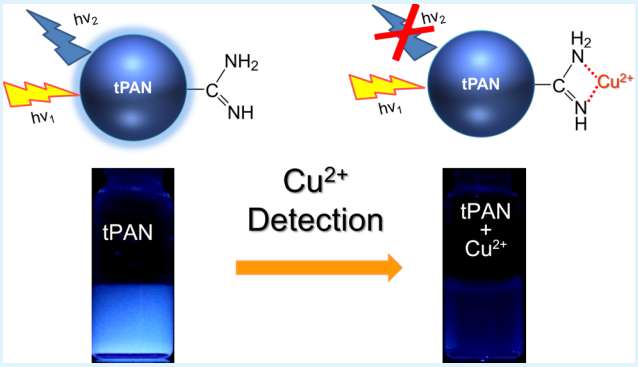

KEYWORDS: *fluorescence, polymer nanoparticle, metal ion sensing, copper ion, cell imaging*

INTRODUCTION

The copper ion, an essential metal ion for human life, is required in various physiological processes and metabolism for all organisms.[1] Copper ion plays important roles in enzymes cofactor, bone formation, cellular respiration, and connective tissue development.[2] However, unlike these bound copper ions, free copper ions can generate reactive oxygen species (ROS), inducing apoptosis in cells.[3,4] Moreover, the accumulation of free copper ions leads to gastrointestinal disturbance, liver or kidney damage, and neurodegenerative diseases such as Alzheimer's, Parkinson's, and prion diseases.[5,6] Therefore, sensitive measurement of copper ions in biological systems and environmental monitoring are important for human health and environmental protection.[7,8]

To detect and visualize free copper ions in living cells, many efforts have been devoted to the fabrication of fluorescent sensor with strong fluorescence and high sensitivity/selectivity.[9−13] In particular, quantum dots (QDs) have received attention as a copper ion sensor probe due to their unique optical properties such as wideband excitation, narrow emission, and high quantum yield.[14,15] The heavy metal ions containing QDs, however, have intrinsic limitations such as potential toxicity, luminescence blinking, and chemical instability.[16] In order to solve these problems, heavy-metal-free QDs such as carbon quantum dots or graphene quantum dots have been fabricated and applied in copper ion sensors. They, as fluorescent probes for copper ions, exhibit better biocompatibility but still have low limit of detection.[17,18] They also have common disadvantages of a complicated synthetic process and functionalization. Hence, novel nanomaterials with low toxicity, high fluorescence, and easy preparation are needed for the detection of copper ions.

As alternatives for QDs, polymer fluorescent nanomaterials have attracted a great deal of interest due to their low cytotoxicity, easy surface functionalization, and high price competitiveness.[19,20] However, they have not been explored until recently due to the difficulty of fabrication of nanostructures.[21] We synthesized fluorescent polyacrylonitrile nanoparticles (PAN NPs) and applied them as bioimaging agents and fluorescent sensor probe for ROS, monosaccharide, and anthrax detection.[19−22] They possessed blue fluorescence, low cytotoxicity, and abundant surface functional groups, which enable their modification using various moieties.[20]

Herein, we fabricated amidine/Schiff base dual-modified PAN NPs (tPAN NP) for copper ion detection in living cells. Both amidine and Schiff base can be introduced on the surface

Received: July 22, 2014
Accepted: September 8, 2014
Published: September 8, 2014

   dx.doi.org/10.1021/am504824n | ACS Appl. Mater. Interfaces 2014, 6, 17151−17156

of the PAN NPs by a simple treatment. Amidine group is well-known as an effective functional ligand for removing copper ions from aqueous solution.[23] Moreover, Schiff base group can enhance the fluorescence of the tPAN NPs. Therefore, amidine/Schiff base modification provides increased fluorescence and excellent detecting performance for the copper ions. To the best of our knowledge, this is the first report using fluorescent polymer nanoparticles for detection of copper ions in vitro.

EXPERIMENTAL SECTION

Materials. Hydrogen chloride and diethyl ether were purchased from Samchun Chemical. The following chemicals purchased from Aldrich: acrylonitrile monomer, dodecylsulfacte, cerium sulfate, nitroacetic acid, ammonia solution, ethylenediaminetetraacetate, $Al(NO_3)_3$, $AgNO_3$, $CdCl_2$, $CoCl_2$, $CuCl_2$, $FeCl_3$, $FeCl_2$, $HgCl_2$, $MgCl_2$, $MnCl_2$, $NiCl_2$, $Pb(NO_3)_2$, $ZnCl_2$, NaCl, KCl, and $CaCl_2$.

Fabrication of Polyacrylonitrile Nanoparticles (PAN NPs). The PAN NPs (50 nm) were fabricated by microemulsion polymerization. To fabricate PAN nanoparticles, acrylonitrile (AN; 1.5 g) monomer was dissolved in distilled water with 0.5 g of sodium dodecyl sulfate (SDS). After the introduction of cerium sulfate and nitroacetic acid, the microemulsion polymerization of the AN monomer proceeded for 10 min. The resulting product was washed with ethanol three times.

Fabrication of Amidine/Schiff Base Modified PAN NPs (tPAN NPs). The tPAN nanoparticles were achieved by surface modification. This was followed by treatment with hydrogen chloride and then ammonia under nitrogen to form amidine and Schiff base groups on the PAN nanoparticles. First, 0.5 g of PAN NPs in ethanol (10 mL) was added into 1 M HCl in diethyl ether (20 mL) at 0 °C for 72 h in round-bottomed flasks under N_2 reflux. Then, the product was washed with ethanol. The product was treated with ammonia solution (20 mL) under a nitrogen purge for 3 h. The product was washed with ethanol three times.

Characterization. The transmission electron microscope (TEM) and scanning electron microscope (SEM) images were taken with a JEOL JEM-2100 and JEOL 6330F, respectively. Fourier transform infrared (FT-IR) spectra were collected with a Thermo Scientific Nicole 6700 FT-IR spectrophotometer. The samples for IR detection were prepared by potassium bromide (KBr) pellet method. The powder sample grounded with KBr was pressed to form a pellet. The pellet samples were investigated by IR spectroscopy transmission mode. The fluorescent emission spectra of tPAN nanoparticles were obtained with a JASCO FP-6500 spectrofluorometer.

Quantum Yield. The quantum yield of tPAN particles was obtained by comparing the fluorescence emission of a reference dye and that of tPAN NPs. 7-Amino-4-methylcoumarin is blue-emitting dye with a high quantum yield (Φ = 0.88), which is used as standard reference. The quantum yield of tPAN particles was calculated by the following equation:

$$\Phi_P = \frac{F_P}{A_P} \times \frac{A_D}{F_D} \times \Phi_D$$

where Φ is the fluorescence quantum yield, F is the integrated area of emitted fluorescence spectra, and A is the absorbance at the excitation wavelength. The subscript P and D implied tPAN particles and 7-amino-4-methylcoumarin, respectively.

Cell Culture. Human breast cancer SK-BR-3 cells (American Type Culture Collection, Manassas, VA) were cultured in RPMI-1640 medium with 10% fetal bovine serum and 1% penicillin-streptomycin solution. They were maintained in a 75T flask at 37 °C in humidified 5% CO_2 atmosphere and passaged at 70−80% confluence.

Observation of tPAN NPs-Treated Cells. SK-BR-3 cells were seeded at a density of 3000 cells per well in 8-well Lab-Tek II chambered coverglass (Nunc, Thermo Fisher Scientific, USA) and inserted with 10 μg mL^{-1} of tPAN NPs. After 24 h, the cells were washed twice with 0.1 M phosphate buffered solution (PBS), and treated with 10 μM $CuCl_2$ for 20 min at 37 °C. As control experiment, excess ethylenediaminetetraacetate (EDTA, 100 μM) was incubated for 20 min to remove Cu^{2+} from the culture medium. The cells were washed again and analyzed with a Delta Vision RT imaging system (Applied Precision, Issaquah, WA). To obtain images, we used a Cascade II electron multiplying charge-coupled device camera.

Viability Test. For cell viability, Cell-Titer glow luminescent cell viability assay (Promega, Madison, WI) was used. SK-BR-3 cells were seeded in white opaque 96-well plates at a density of 1.5 × 10^4 cells mL^{-1} for 24 h, and various concentration of tPAN NPs (5, 10, 50, 100, and 250 μg mL^{-1}) were inserted for another 24 h. Then, the culture medium was eliminated, and following steps were performed by manufacturer's instructions. The luminescence (595 nm) was detected by Victor3Multilabel Readers (PerkinElmer, Boston, MA). The viability was calculated by dividing the ATP content of tPAN NPs-treated cells by that of untreated cells (negative control).

ROS Production. For the measurement of ROS, 2′,7′-dichlorodihydrofluorescein diacetate (H2DCF-DA; Invitrogen, Grand Island, NY) staining was performed. SK-BR-3 cells were spread in black opaque 96-well plates at a concentration of 1.5 × 10^4 cells mL^{-1} for 24 h and treated with tPAN NPs (5, 10, 50, 100, and 250 μg mL^{-1}) for another 24 h. They were washed with 0.1 M Hank's buffered salt solution and treated with 10 μM H2DCF-DA for 30 min at 37 °C. Fluorescence intensity was detected by Victor3Multilabel Readers (λ_{ex} = 485 nm, λ_{em} = 535 nm).

RESULTS AND DISCUSSION

PAN NPs were fabricated by ultrasonic mediated emulsion polymerization, as reported previously.[14] Ultrasonic irradiation formed emulsion phase by dissolving sodium dodecyl sulfate and acrylonitrile monomer in distilled water. After introducing cerium sulfate and nitroacetic acid into the solution as co-initiators, additional ultrasound was administered for the polymerization of acrylonitrile monomer. AS shown in Scheme 1, as-prepared PAN NPs were modified by hydrogen chloride

Scheme 1. Schematic Diagram of Fabrication of tPAN NPs

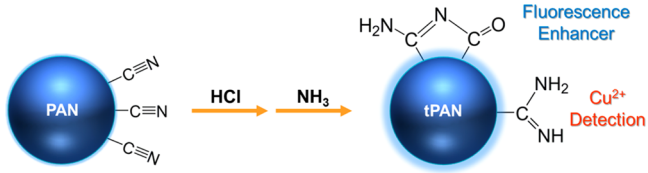

and ammonia under nitrogen purge. Fabrication of the PAN NPs and their surface modification do not require complicated procedures and careful regulation of temperature, as opposed to the preparation of QDs.[14−17] Due to the change of the surface functional group, tPAN NPs can detect copper ions by amidine group, and Schiff base can enhance the fluorescence of tPAN NPs. The PAN and tPAN NPs had a narrow size distribution, largely in the range of 40−50 nm as determined by TEM and SEM images (Figure 1). Furthermore, high-resolution TEM (HRTEM) images (Figure S1, Supporting Information) showed that the shape and size of PAN NPs and tPAN NPs were still maintained after surface modification.

Formation of the PAN NPs and the tPAN NPs was confirmed by FT-IR spectrometry (Figure 2). FT-IR spectra of the PAN NPs showed characteristic PAN peaks, including the C≡N stretching bands at 2244 cm^{-1}, the C−H stretching peak at 2948 cm^{-1}, and the C−H deformation peak at 1451 cm^{-1}. These peaks revealed successful polymerization of the PAN NPs by ultrasonic mediated emulsion polymerization. For the tPAN NPs, new double peaks related to the primary amine

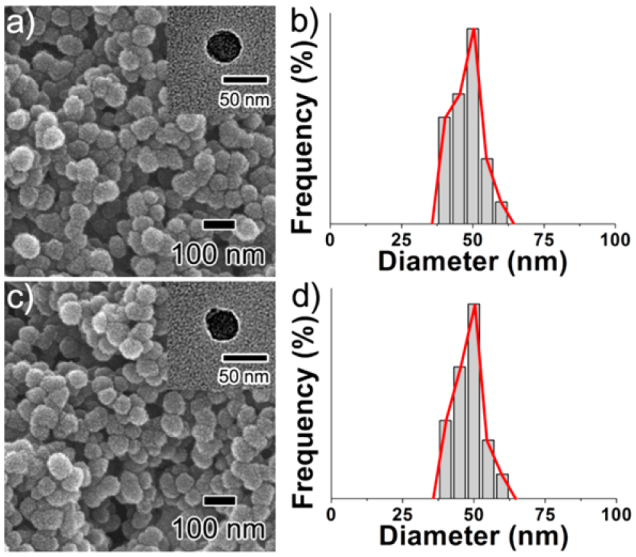

Figure 1. (a and c) SEM images (insets, TEM images) and (b and d) size distribution histograms of (a and b) PAN NPs and (c and d) tPAN NPs.

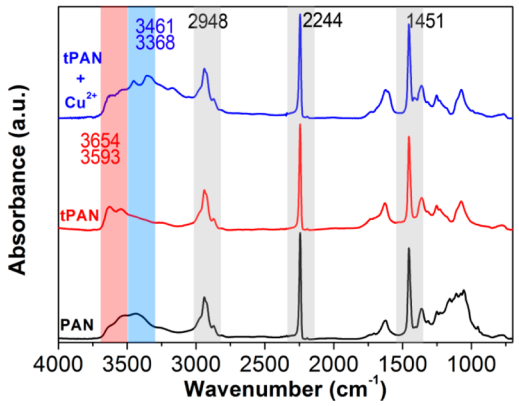

Figure 2. FT-IR spectra of (black) PAN NPs, (red) tPAN NPs, and (blue) tPAN NPs + Cu^{2+}.

group appeared, including peaks at 3593 and 3654 cm^{-1}. The peaks related to Schiff base increased, including the Schiff base peak at 1626 cm^{-1} and C═O stretching at 1730 cm^{-1}.[19] On the basis of these data, amidine/Schiff base were successfully introduced on the PAN NPs surfaces.

The optical properties of PAN NPs and tPAN NPs were studied by UV−vis absorption and photoluminescence (PL) spectroscopy. The UV−vis absorption spectrum of the tPAN NPs had absorption enhancement in the UV region (200−300 nm) with a peak at 260 nm, compared to that of the PAN NPs (Figure 3). This 260 nm band peak represented a $\pi-\pi^*$ transition of the C═N group, which is in accordance with FT-IR data.[20] Inset images in Figure 3 illustrate the fluorescence color change from blue (PAN NPs) to bright blue (tPAN NPs) by surface modification. The fluorescence intensity of the tPAN NPs is 11 times higher than that of the PAN NPs (Figure 4a). Their fluorescence quantum yield was calculated as ca. 0.19 using the standard reference 7-amino-4-methylcoumarin, which is also higher than that of the PAN NPs.[19,22,24,25] The increased fluorescence of the tPAN NPs is caused by Schiff base on the surface of the tPAN NPs, which is consistent with other precedent research (Figure S2, Supporting Information).[26,27]

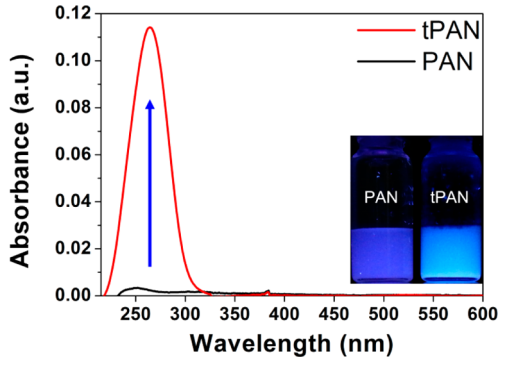

Figure 3. UV−vis absorption spectra of PAN NP and tPAN NPs. (Inset) Photographs of PAN NPs and tPAN NPs under UV light (365 nm).

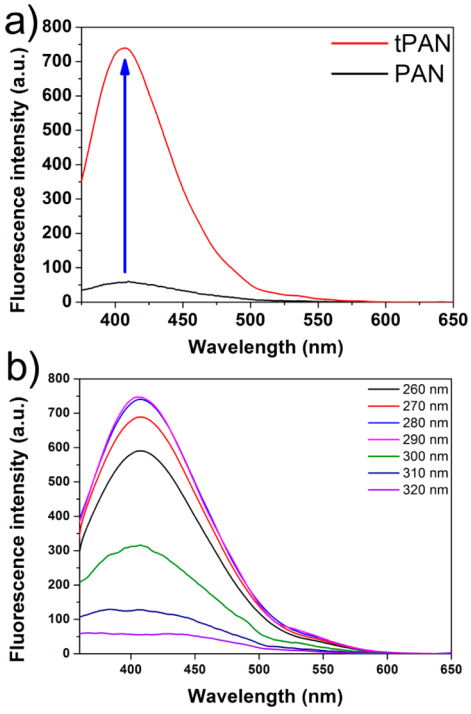

Figure 4. (a) Fluorescence spectra of PAN NP and tPAN NPs. (b) Fluorescence spectra of tPAN NPs under different excitation wavelength.

We further analyzed excitation dependent emission of the tPAN NPs by changing excitation wavelength from 260 to 320 nm (Figure 4b). The maximum emission intensity of the tPAN NPs was achieved at 410 nm (λ_{ex} = 290 nm), which is optimal excitation wavelength for the experiments. Considering these data, tPAN NPs can be used as an intracellular fluorescence sensing probe due to enhanced PL properties.

To identify the capability of the tPAN NPs as sensor for copper ion, we evaluated the selectivity of the tPAN NPs by screening various metal ions at a concentration of 10 μM (Figure 5a). The fluorescence of the tPAN NPs was only quenched by the addition of copper ions (26% quenching upon addition of 10 μM Cu^{2+}), while no significant quenching effect was observed with other metal ions (Ag^+, Al^{3+}, Ca^{2+}, Cd^{2+}, Co^{2+}, Fe^{2+}, Fe^{3+}, Hg^{2+}, K^+, Mg^{2+}, Mn^{2+}, Na^+, Ni^+, Pb^{2+}, and Zn^{2+}). In general, copper ions have a tendency to be coordinated with amidine group due to unshared electrons of the nitrogen atoms on the amidine group.[23,28] Because of its

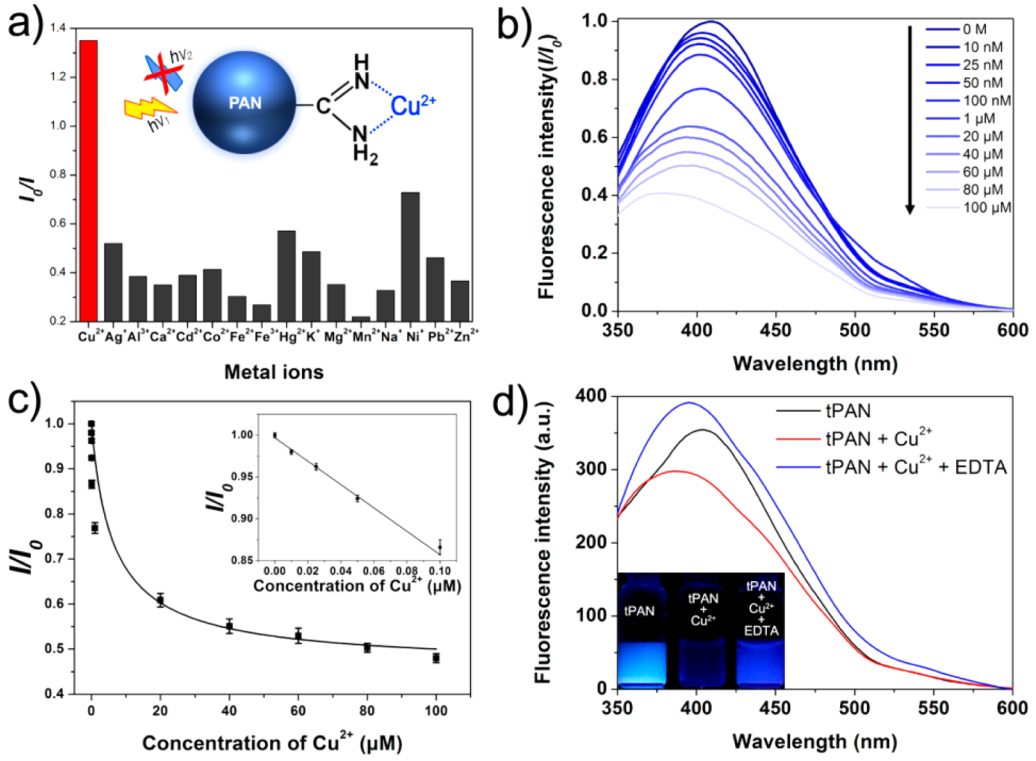

Figure 5. (a) Selectivity of tPAN NPs (10 μg mL^{-1}) for different metal ions (10 μM), (inset) possible sensing mechanism of tPAN NP for Cu^{2+}. (b) Fluorescence emission spectra of tPAN NPs in the presence of Cu^{2+} at different concentrations (0−100 μM). (c) On the basis of the Figure 5b, the relationship between emission fluorescence intensity of tPAN NPs and concentrations of Cu^{2+} was calculated. I and I_0 are the emission fluorescence intensities of the tPAN NPs at 410 nm (λ_{ex} = 290 nm) in the presence and absence of Cu^{2+}, respectively; (inset) the linear region. (d) Representative fluorescence spectra with the addition of Cu^{2+} and EDTA in the quenching recovering; (inset) fluorescence photographs of tPAN NPs, tPAN NPs + Cu^{2+}, and tPAN NPs + Cu^{2+} + EDTA under UV light (365 nm).

paramagnetic property and unfilled d shell, only copper ion could strongly quench the fluorescence of the tPAN NPs through electron transfer processes.[29−31] To determine the interference effect of tPAN NPs coexisting with other metal ions in copper ion detection, we investigated the effect of other metal ions on the fluorescence intensity (Figure S3, Supporting Information), and we found that the emission intensity of the tPAN NPs to copper ions was almost unchanged in the presence of other metal ions. The interaction between tPAN NPs and copper ions was confirmed by FT-IR analysis. Figure 2 revealed that the peaks of tPAN NPs at 3593 and 3654 cm^{-1} were shifted to 3368 and 3461 cm^{-1} after copper ion treatment. These changes meant free copper ions were bound with the primary amine groups on the surface of the tPAN NPs. The C≡N bond at the 2244 cm^{-1} was not changed, implying that the nitrile group on the tPAN NPs was not included in the detection of copper ions. However, as shown in Figure S4 (Supporting Information), there are no peak shifts of tPAN NPs after the addition of some metal ions (Fe^{2+}, Fe^{3+}, Hg^{2+}, and Zn^{2+}), which indicates that copper ions have higher binding affinity with amidine group on the surface of tPAN NPs than other metal ions. The interaction between tPAN NPs and metal ions was also studied by UV−vis absorption (Figure S5, Supporting Information). The binding ability of tPAN NPs with various metal ions (Ag^{+}, Al^{3+}, Ca^{2+}, Cd^{2+}, Co^{2+}, Fe^{2+}, Fe^{3+}, Hg^{2+}, K^{+}, Mg^{2+}, Mn^{2+}, Na^{+}, Ni^{+}, Pb^{2+}, and Zn^{2+}) showed a selective response toward Cu^{2+} ions. As shown in Figure S5 (Supporting Information), the addition of Cu^{2+} resulted in a significant change indicating that the tPAN NPs have higher binding affinity toward Cu^{2+} than other metal ions. All these results demonstrate that the tPAN NPs are highly selective for copper ion detection. On the basis of these analyses, possible interaction between tPAN NPs and copper ions is depicted in the inset images in Figure 5a. As displayed in Figure 5b, the fluorescence intensity of the tPAN NPs (10 μg mL^{-1}) decreased by adding copper ions, and the peak was blue-shifted from 410 to 370 nm (λ_{ex} = 290 nm). On the basis of Figure 5b, fluorescence intensity change of the tPAN NPs was calculated versus copper ion concentration (Figure 5c). The fluorescence intensity remarkably decreased with increasing copper ion concentration. The inset graph showed a linear correlation between the emission intensities and the concentration of copper ions (0−100 nM; adjusted R^2 = 0.991). The limit of detection was 10 nM (3σ of the reagent blank signal), which is 2−3 orders of magnitude lower than previous reports.[17,18] Additionally, in the physiological concentrations, the minimum concentration of intracellular copper ions is 10 μM, suggesting that the tPAN NPs are suitable as a sensitive detection probe for copper ions under the physiological conditions.[17] As a control experiment, ethylenediaminetetraacetate (EDTA) was inserted into the solution containing copper ions and tPAN NPs (Figure 5d). EDTA can chelate with metal ions in a 1:1 ratio, which induces removal of the metal ions from the solution.[31] The quenched fluorescence of the tPAN NPs in the presence of copper ion was recovered into strong fluorescence by EDTA treatment (inset images in Figure 5d). Taking these facts into account, tPAN NPs are proper sensors for copper ion detection with high sensitivity and selectivity against other metal ions.

The sensing ability of the tPAN NPs was systematically investigated in vitro. SK-BR-3 cells were incubated with 10 μg mL^{-1} tPAN NPs for 24 h (Figure 6a). The amidine group of

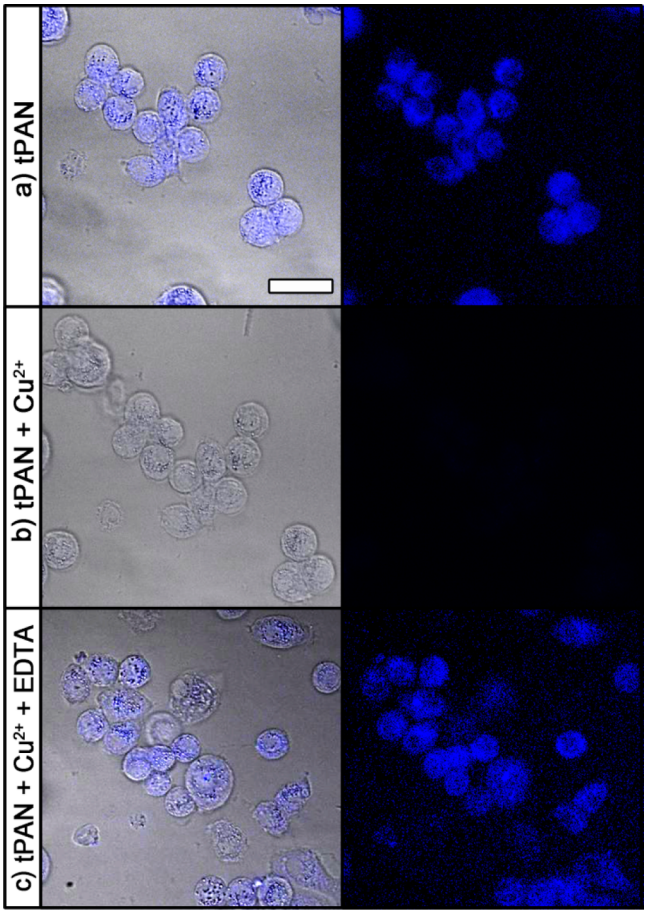

Figure 6. Live cell differential interference images of tPAN NPs-treated SK-BR-3 cells; (a) before treatment of Cu^{2+}, (b) 20 min after treatment of 10 μg/mL Cu^{2+}, and (c) 20 min after treatment of 100 μg/mL EDTA. Scale bars = 50 μm.

the tPAN NPs possess a positive surface charge, leading to adhesion between tPAN NPs and the plasma membrane of the cells.[32] Internalized tPAN NPs exhibited blue fluorescence in the cytoplasm, making tPAN NPs possible to detect copper ions in cells. Then, the copper ions were inserted into the culture medium for 20 min, and the blue fluorescence of the tPAN NPs was turned off in the presence of copper ions (Figure 6b). Upon addition of the same concentration of copper ions (Figure S6, Supporting Information), the intensity of the blue emission from the tPAN NPs distinctively decreased, which agreed well with a change of the blue fluorescence observed in SK-BR-3 cells. Then, excess EDTA was added to the culture medium containing copper ions in order to eliminate copper ions. The strong fluorescence of tPAN NPs reappears, as shown in Figure 6c. These data implies that tPAN NPs is easily introduced into cells and can be used as a fluorescence sensor for copper ions in living cells.

Low cytotoxicity of the tPAN NPs is required for the use of tPAN NPs as an intracellular sensor probe. Cytotoxicity of the tPAN NPs was determined by two methods (Figure 7); adenosine triphosphate (ATP) based viability test and generation of ROS by tPAN NP treatment. First, ATP

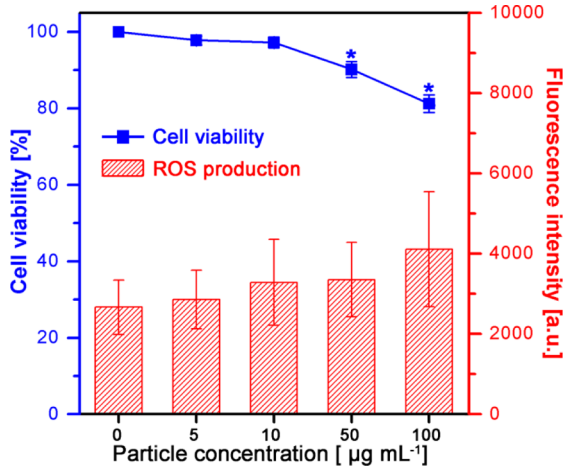

Figure 7. (Blue) Viability of SK-BR-3 cells incubated with tPAN nanoparticles for 24 h. The viability was calculated relative to a negative control. (Red) ROS production by SK-BR-3 cells after being incubated with tPAN. H_2O_2 (0.02%) was used as a positive control. Values exhibit mean ± SD, and each experiment was performed in triplicate.

concentrations of tPAN NP treated SK-BR-3 cells were measured by transformation of luciferin to oxyluciferin. Until a concentration of 10 μg mL^{-1}, tPAN NPs have no significant effect on the cell viability. The viability was over 80%, even at a high concentration of the tPAN NPs (100 μg mL^{-1}) for 24 h incubation. We also evaluate production of ROS in tPAN NP-added SK-BR-3 cells by 2′,7′-dichlorodihydrofluorescein diacetate (H_2DCF-DA) staining. After tPAN NP treatment, compared to the negative control, ROS production increased within the margin of error. Collectively, tPAN NPs can be applied as an intracellular copper ion detector without significant viability decrease or ROS production. Therefore, tPAN NPs offer a selective detection probe for copper ion in living cells with low toxicity.

CONCLUSIONS

In conclusion, amidine/Schiff base dual-modified PAN nanoparticles (tPAN NPs) were fabricated for the sensitive and selective detection of free copper ions in vitro. PAN NPs were synthesized by sonication mediated emulsion polymerization, and further modified with amidine/Schiff base through hydrogen chloride and ammonia treatment without careful regulation of temperature. The tPAN NPs exhibited excellent selectivity for copper ions in aqueous solution and mammalian cells, based on the quenching effect. Moreover, the detection limit of the tPAN NPs is improved, compared with other strategies for Cu^{2+} detection. Considering these observations, the fluorescent tPAN NPs with biocompatibility offer a new direction for selective recognition of copper ions in living cells.

ASSOCIATED CONTENT

Supporting Information

Schematic diagram of Schiff base reaction. This material is available free of charge via the Internet at http://pubs.acs.org.

AUTHOR INFORMATION

Corresponding Author

*E-mail: jsjang@plaza.snu.ac.kr.

Author Contributions

†These authors contributed equally to this work.

Notes

The authors declare no competing financial interest.

■ ACKNOWLEDGMENTS

This research was supported by a World Class University (WCU) program through the National Research Foundation of Korea funded by the Ministry of Education, Science and Technology (R31-10013).

■ REFERENCES

(1) Kim, K. B.; Kim, H.; Song, E. J.; Kim, S.; Noh, I.; Kim, C. A Cap-Type Schiff base Acting as a Fluorescence Sensor for Zinc(II) and a Colorimetric Sensor for Iron(II), Copper(II), and Zinc(II) in Aqueous Media. *Dalton Trans.* **2013**, *42*, 16569−16577.

(2) Viguier, R. F. H.; Hulme, A. N. A Sensitized Europium Complex Generated by Micromolar Concentrations of Copper(I): Toward the Detection of Copper(I) in Biology. *J. Am. Chem. Soc.* **2006**, *128*, 11370−11371.

(3) Barnham, K. J.; Masters, C. L.; Bush, A. I. Neurodegenerative Diseases and Oxidative Stress. *Nat. Rev. Drug Discovery* **2004**, *3*, 205−214.

(4) Jomova, K.; Valko, M. Advances in Metal-Induced Oxidative Stress and Human Disease. *Toxicology* **2011**, *283*, 65−87.

(5) Geng, J.; Li, M.; Wu, L.; Ren, J.; Qu, X. Liberation of Copper from Amyloid Plaques: Making a Risk Factor Useful for Alzheimer's Disease Treatment. *J. Med. Chem.* **2012**, *55*, 9146−9155.

(6) Nguyen, M.; Robert, A.; Sournia-Saquet, A.; Vendier, L.; Meunier, B. Characterization of New Specific Copper Chelators as Potential Drugs for the Treatment of Alzheimer's Disease. *Chem.—Eur. J.* **2014**, *20*, 6771−6785.

(7) Jeong, Y.; Yoon, J. Recent Progress on Fluorescent Chemosensors for Metal Ions. *Inorg. Chim. Acta* **2012**, *381*, 2−14.

(8) Sarkar, S.; Chatti, M.; Mahalingam, V. Highly Luminescent Colloidal Eu^{3+}-Doped $KZnF_3$ Nanoparticles for the Selective and Sensitive Detection of Cu^{II} Ions. *Chem.—Eur. J.* **2014**, *20*, 3311−3316.

(9) Qu, Q.; Zhu, A.; Shao, X.; Shi, G.; Tian, Y. Development of a Carbon Quantum Dots-Based Fluorescent Cu^{2+} Probe Suitable for Living Cell Imaging. *Chem. Commun.* **2012**, *48*, 5473−5475.

(10) Sun, H.; Gao, N.; Wu, L.; Ren, J.; Wei, W.; Qu, X. Highly Photoluminescent Amino-Functionalized Graphene Quantum Dots Used for Sensing Copper Ions. *Chem.—Eur. J.* **2013**, *19*, 13362−13368.

(11) You, Q.-H.; Lee, A. W.-M.; Chan, W.-H.; Zhu, X.-M.; Leung, K. C.-F. A Coumarin-Based Fluorescent Probe for Recognition of Cu^{2+} and Fast Detection of Histidine in Hard-to-Transfect Cells by a Sensing Ensemble Approach. *Chem. Commun.* **2014**, *50*, 6207−6210.

(12) Xing, C.; Hao, C.; Liu, L.; Xu, C.; Kuang, H. A Highly Sensitive Enzyme-Linked Immunosorbent Assay for Copper(II) Determination in Drinking Water. *Food Agric. Immunol.* **2013**, *25*, 432−442.

(13) Xing, C.; Feng, M.; Hao, C.; Xu, L.; Wang, L.; Xu, C. Visual Sensor for the Detection of Trace Cu(II) Ions using an Immunochromatographic Strip. *Immunol. Invest.* **2013**, *42*, 221−234.

(14) Wu, D.; Chen, Z.; Huang, G.; Liu, X. ZnSe Quantum Dots Based Fluorescence Sensors for Cu^{2+} Ions. *Sens. Actuators, A* **2014**, *205*, 72−78.

(15) Zhao, J.; Deng, J.; Yi, Y.; Li, H.; Zhang, Y.; Yao, S. Label-Free Silicon Quantum Dots as Fluorescent Probe for Selective and Sensitive Detection of Copper Ions. *Talanta* **2014**, *125*, 372−377.

(16) Derfus, A. M.; Chan, W. C. W.; Bhatia, S. N. Probing the Cytotoxicity of Semiconductor Quantum Dots. *Nano Lett.* **2003**, *4*, 11−18.

(17) Zhu, A.; Qu, Q.; Shao, X.; Kong, B.; Tian, Y. Carbon-Dot-Based Dual-Emission Nanohybrid Produces a Ratiometric Fluorescent Sensor for in Vivo Imaging of Cellular Copper Ions. *Angew. Chem., Int. Ed.* **2012**, *51*, 7185−7189.

(18) Salinas-Castillo, A.; Ariza-Avidad, M.; Pritz, C.; Camprubi-Robles, M.; Fernandez, B.; Ruedas-Rama, M. J.; Megia-Fernandez, A.; Lapresta-Fernandez, A.; Santoyo-Gonzalez, F.; Schrott-Fischer, A.; Capitan-Vallvey, L. F. Carbon Dots for Copper Detection With Down and Upconversion Fluorescent Properties as Excitation Sources. *Chem. Commun.* **2013**, *49*, 1103−1105.

(19) Lee, K. J.; Oh, W.-K.; Song, J.; Kim, S.; Lee, J.; Jang, J. Photoluminescent Polymer Nanoparticles for Label-Free Cellular Imaging. *Chem. Commun.* **2010**, *46*, 5229−5231.

(20) Oh, W. K.; Jeong, Y. S.; Song, J.; Jang, J. Fluorescent Europium-Modified Polymer Nanoparticles for Rapid and Sensitive Anthrax Sensors. *Biosens. Bioelectron.* **2011**, *29*, 172−177.

(21) Oh, W.-K.; Jeong, Y. S.; Lee, K. J.; Jang, J. Fluorescent Boronic Acid-Modified Polymer Nanoparticles for Enantioselective Monosaccharide Detection. *Anal. Methods* **2012**, *4*, 913−918.

(22) Lee, K. J.; Oh, J. H.; Kim, Y.; Jang, J. Fabrication of Photoluminescent-Dye Embedded Poly(methyl methacrylate) Nanofibers and Their Fluorescence Resonance Energy Transfer Properties. *Adv. Mater.* **2006**, *18*, 2216−2219.

(23) Deng, S.; Bai, R.; Chen, J. P. Behaviors and Mechanisms of Copper Adsorption on Hydrolyzed Polyacrylonitrile Fibers. *J. Colloid Interface Sci.* **2003**, *260*, 265−272.

(24) Oh, W. K.; Jeong, Y. S.; Kim, S.; Jang, J. Fluorescent Polymer Nanoparticle for Selective Sensing of Intracellular Hydrogen Peroxide. *ACS Nano* **2012**, *6*, 8516−8524.

(25) Yang, L.; Zhu, W.; Fang, M.; Zhang, Q.; Li, C. A New Carbazole-based Schiff Base as Fluorescent Chemosensor for Selective Detection of Fe^{3+} and Cu^{2+}. *Spectrochim. Acta, Part A* **2013**, *109*, 186−192.

(26) Huang, S.-H.; Jiang, G. J.; Liaw, D.-J.; Li, C.-L.; Hu, C.-C.; Lee, K.-R.; Lai, J.-Y. Effects of the Polymerization and Pervaporation Operating Conditions on the Dehydration Performance of Interfacially Polymerized Thin-Film Composite Membranes. *J. Appl. Polym. Sci.* **2009**, *114*, 1511−1522.

(27) Lee, M. H.; Giap, T. V.; Kim, S. H.; Lee, Y. H.; Kang, C.; Kim, J. S. A Novel Strategy to Selectively Detect Fe(III) in Aqueous Media Driven by Hydrolysis of a Rhodamine 6G Schiff Base. *Chem. Commun.* **2010**, *46*, 1407−1409.

(28) Kampalanonwat, P.; Supaphol, P. Preparation and Adsorption Behavior of Aminated Electrospun Polyacrylonitrile Nanofiber Mats for Heavy Metal Ion Removal. *ACS Appl. Mater. Interfaces* **2010**, *2*, 3619−3627.

(29) Li, Z.; Zhang, L.; Wang, L.; Guo, Y.; Cai, L.; Yu, M.; Wei, L. Highly Sensitive and Selective Fluorescent Sensor for Zn^{2+}/Cu^{2+} and New Approach for Sensing Cu^{2+} by Central Metal Displacement. *Chem. Commun.* **2011**, *47*, 5798−5800.

(30) Hong, Y.; Chen, S.; Leung, C. W. T.; Lam, J. W. Y.; Liu, J.; Tseng, N.-W.; Kwok, R. T. K.; Yu, Y.; Wang, Z.; Tang, B. Z. Fluorogenic Zn(II) and Chromogenic Fe(II) Sensors Based on Terpyridine-Substituted Tetraphenylethenes with Aggregation-Induced Emission Characteristics. *ACS Appl. Mater. Interfaces* **2011**, *3*, 3411−3418.

(31) Muhammed, M. A. H.; Verma, P. K.; Pal, S. K.; Retnakumari, A.; Koyakutty, M.; Nair, S.; Pradeep, T. Luminescent Quantum Clusters of Gold in Bulk by Albumin-Induced Core Etching of Nanoparticles: Metal Ion Sensing, Metal-Enhanced Luminescence, and Biolabeling. *Chem.—Eur. J.* **2010**, *16*, 10103−10112.

(32) Tang, R.; Ji, W.; Wang, C. Synthesis and Characterization of New Ooly(ortho ester amidine) Copolymers for Non-Viral Gene Delivery. *Polymer* **2011**, *52*, 921−932.